

The 5th International Conference of Euro Asia Civil Engineering Forum (EACEF-5)

## Testing of the kriging-based finite element to shell structures with varying thickness

Foek Tjong Wong<sup>a,\*</sup>, Yosua Christabel<sup>b</sup>, Pamuda Pudjisuryadi<sup>a</sup>,  
Worsak Kanok-Nukulchai<sup>c</sup>

<sup>a</sup>*Petra Christian University, Jl. Siwalankerto 121-131, Surabaya 60236, Indonesia*

<sup>b</sup>*Benjamin Gideon and Associates, Jl. Gayungsari VII 30-32, Surabaya 60235, Indonesia*

<sup>c</sup>*Asian Institute of Technology, Khlong Luang P.O. Box 4, Pathumthani 12120, Thailand*

---

### Abstract

A variant of the finite element method with Kriging basis functions has been recently developed and applied to plane, plate bending, and shell elastostatic problems. The main advantage of this novel method is that high degree of basis functions can be easily constructed without additional finite element nodes (such as mid-side and inner nodes). This paper revisits the formulation of the Kriging-based finite element method for analysis of curved shell structures, referred to as K-Shell, and presents new numerical tests to shell structures with varying thickness. The K-Shell was formulated based on degenerated 3D elasticity theory. The basis functions were constructed using a set of nodes covering several layers of triangular elements and were employed to approximate both the displacement and geometry. The quartic polynomial basis was chosen to alleviate shear and membrane locking. The K-Shell has been tested using a series of shell benchmark problems with constant shell thickness. The tests showed that K-Shell performed very well in analyzing moderately thick smooth shells. In this paper the K-Shell is tested using two modified shell benchmark problems with varying thickness, i.e. the modified pinched cylinder and the modified hemispherical shell with 18 degrees cut-off. The converged results of three-dimensional finite element model using commercial software Abaqus were used to assess the convergence of the results. The tests show that the performance of K-Shell in analyzing shells with varying thickness is satisfactory.

© 2015 The Authors. Published by Elsevier Ltd. This is an open access article under the CC BY-NC-ND license (<http://creativecommons.org/licenses/by-nc-nd/4.0/>).

Peer-review under responsibility of organizing committee of The 5th International Conference of Euro Asia Civil Engineering Forum (EACEF-5)

**Keywords:** finite element; shell, Kriging, benchmark problem, varying thickness

---

---

\* Corresponding author.

E-mail address: [wftjong@petra.ac.id](mailto:wftjong@petra.ac.id)

## 1. Introduction

A new variant of the finite element method (FEM) with Kriging interpolation (KI), referred to as Kriging-based finite element method (K-FEM), was proposed by Plengkhom & Kanok-Nukulchai [1]. In this method, the “element-by-element” piecewise KI is employed for approximating the unknown functions of a boundary value problem, in place of conventional polynomial interpolation [2,3]. For each element, KI is constructed from a set of nodes within a prescribed support domain comprising the element and its several layers of adjacent elements. The key advantages of the K-FEM are a high degree polynomial interpolation can be easily incorporated even using the simplest elements such as a three-node triangle. Furthermore, the formulation and algorithm are very similar to the conventional FEM so that it can be incorporated in an existing FE code without major change.

A shortcoming of the K-FEM is that the interpolation function is discontinuous over the elements’ boundary. The effect of the discontinuity on the convergence of solutions has been numerically studied using several numerical tests, including the patch test [4]. The study showed that the solutions of the K-FEM with appropriate interpolation parameters converged to the exact solutions in spite of the discontinuity.

It is worthy to note several recent literatures using KI as the approximation function for different problems. Bui et al. [5,6,7] presented moving Kriging interpolation-based meshfree methods for 2D elastodynamic analysis, Kirchhoff plate free-vibration analysis, and Reissner-Mindlin plate buckling analysis. The so-called moving Kriging-based meshfree method, specifically the element-free Galerkin method (EFGM) with moving KI [8], is essentially a class of the meshfree method of which the K-FEM is originated [2,3]. The K-FEM is indeed a more convenient implementation of the Kriging-based EFGM: In the K-FEM, the EFGM support domain for each point in an element is chosen to be a polygon made from the element and several layers of adjacent elements. Moreover, the elements serve as the EFGM background cells for performing numerical integration. Accordingly the K-FEM can be viewed as a variant of the Kriging-based EFGM.

The K-FEM has been further developed and applied for analysis of shell structures [9,10,11]. The development of the shell element was based on the degenerated 3D elasticity theory. The KI was constructed using a set of nodes encompassing four layers of triangular elements. The KI was used to approximate both the displacement field and the geometry of the shell. The quartic polynomial function was included in the KI in order to alleviate shear and membrane locking. The developed curved triangular Kriging-based shell element is referred to as K-Shell. The K-Shell has been tested using a number of benchmark shell problems to evaluate the accuracy, convergence and versatility [10]. The results showed that the element perform very well for moderately thick shells. Actually the K-Shell has the capability to analyze shell structures with varying thickness. However, all of the benchmark problems used were smooth shells with constant thickness. The question is how about the performance of the K-Shell in analyzing structures with varying thickness.

This paper presents an overview of the formulation of the K-Shell and testing of the K-Shell to shell problems with varying thickness. The varying-thickness shell problems were created by modifying the thickness of the well-known shell benchmark problems, specifically the pinched cylinder with end diaphragms and the hemispherical shell with 18° cut-off. The convergence of the K-Shell solutions were assessed by comparing them to the converged results of 3D finite element model using commercial software Abaqus [12].

## 2. Kriging-based Curved Triangular Shell Element (K-Shell)

The variational equation governing a shell motion at a time  $t$ ,  $t \geq 0$  may be written as

$$\int_V \delta \mathbf{u}^T \rho \ddot{\mathbf{u}} dV + \int_V \delta (\boldsymbol{\epsilon}^l)^T \boldsymbol{\sigma}^l dV = \int_{S_p} \delta \mathbf{u}^T \mathbf{p} dS \quad (1)$$

where  $\mathbf{u}$  is the displacement vector of any point  $P$  in the shell,  $\ddot{\mathbf{u}}$  is the corresponding acceleration vector,  $\boldsymbol{\epsilon}^l$  is the vector of shell strain components,  $\boldsymbol{\sigma}^l$  is the vector of shell stress components,  $\rho$  is the mass density of the shell material, and  $\mathbf{p}$  is the time-varying surface force vector (per unit surface area). The operator  $\delta$  denotes the first variation operated on the associated field variable. The integration over  $V$  signifies integration over the shell volume, and the integration over  $S_p$  signifies integration over the surface upon which the surface vector  $\mathbf{p}$  is applied. The components of  $\mathbf{u}$ ,  $\ddot{\mathbf{u}}$ , and  $\mathbf{p}$  vectors are written with respect to the global Cartesian coordinate system, whereas the

components of  $\boldsymbol{\varepsilon}^l$  and  $\boldsymbol{\sigma}^l$  are in the corresponding local or lamina coordinate system [10,13]. The local or lamina coordinate system is the coordinate system introduced at a point to for the purpose of invoking Reissner-Mindlin assumptions.

For the purpose of defining the geometry of the shell, a Cartesian coordinate system is introduced for each curved-triangular element at the centroid of the flat triangle passing through the element nodes (the projected triangle). The geometry of a typical curved-triangular element is described with reference to the element coordinate system by Eqs. (2)-(4).

$$\mathbf{x}^e(\xi, \eta, \zeta) = \bar{\mathbf{x}}^e(\xi, \eta) + \mathbf{X}^e(\xi, \eta, \zeta) \quad (2)$$

$$\bar{\mathbf{x}}^e(\xi, \eta) = \begin{Bmatrix} \bar{x}_1^e \\ \bar{x}_2^e \\ \bar{x}_3^e \end{Bmatrix} = \begin{Bmatrix} \xi \\ \eta \\ \sum_{a=1}^n N_a(\xi, \eta) \bar{x}_{a3}^e \end{Bmatrix} \quad (3)$$

$$\mathbf{X}^e(\xi, \eta, \zeta) = \sum_{a=1}^n N_a(\xi, \eta) \frac{h_{fa}}{2} \zeta \hat{\mathbf{X}}_a^e \quad (4)$$

In these equations,  $\mathbf{x}^e$  denotes the position vector of a point within the shell element;  $\bar{\mathbf{x}}^e$  is the position vector of the point on the mid-surface;  $\mathbf{X}^e$  is a position vector based at  $\bar{\mathbf{x}}^e$ , which defines the “fiber direction” through the point;  $\xi$  and  $\eta$  are surface parameters for defining the mid-surface (*not* natural coordinates as in the conventional isoparametric element);  $\zeta \in [-1, 1]$  is a thickness parameter;  $\bar{x}_{a3}^e$  is the third component of coordinate of node  $a$ ;  $N_a(\xi, \eta)$  denotes a two-dimensional Kriging shape function associated with node  $a$ ;  $h_{fa}$  is the thickness of the shell at node  $a$ , measured in the fiber direction at node  $a$ ; and  $\hat{\mathbf{X}}_a^e$  is a unit vector emanating from node  $a$  in the fiber direction. The summation runs from  $a=1$  until  $a=n$ , where  $n$  is the number of nodes in the element support domain. It should be noted here that  $n$  is *not* the number of element nodes as in the conventional FEM. The superscript  $e$  is used to emphasize that the vector components are in the elemental coordinate system. The thickness in the fiber direction,  $h_{fa}$ , for each node is calculated using the top and bottom coordinates at the associated node. This is the reason why the K-Shell is capable to analyse shells with smoothly varying thickness.

Eq. (3) is the vector equation of the mid-surface. It projects (maps) the points on the mid-surface into the plane passing through the three nodal points. Eqs.(2) through (4) represent a smooth mapping of “projected plate”, whose thickness is bi-unit and whose mid-surface lying in the  $\bar{x}_1^e$ - $\bar{x}_2^e$  plane, into the physical shell domain as illustrated in Fig. 1. With this point of view, parameters  $\xi, \eta, \zeta$  may be viewed as curvilinear coordinates. For  $\zeta$  fixed, the surface defined by Eq. (2) is called a *lamina* and  $\zeta=0$  represents the mid-surface. For  $(\xi, \eta)$  fixed, the line defined by Eq. (2) is called the *fiber*. The fibers are generally not perpendicular to the laminae.

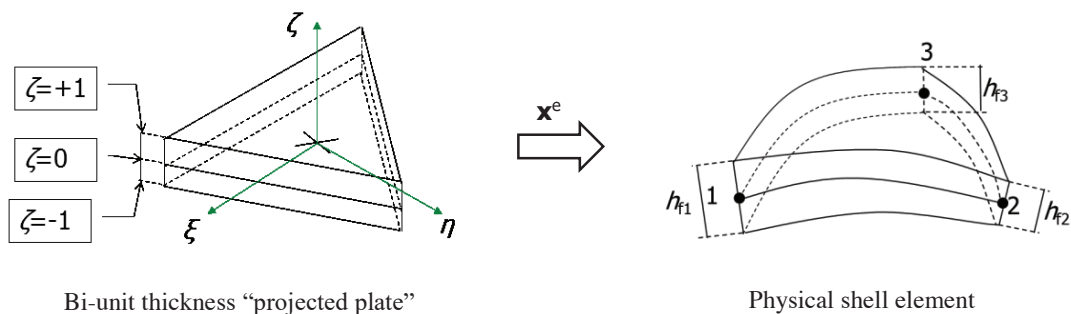


Fig. 1. An illustration for mapping from “projected plate” into physical shell element domain.

The displacement of a generic point in the shell,  $\mathbf{u}(\xi, \eta, \zeta)$ , is decomposed into two parts: the displacement of the projected point on the mid-surface,  $\bar{\mathbf{u}}(\xi, \eta)$ , and the displacement induced by the fiber rotation,  $\mathbf{U}(\xi, \eta, \zeta)$ . The mid-surface displacement and the rotation-induced displacement are approximated from their respective nodal values using KI as follows:

$$\mathbf{u}(\xi, \eta, \zeta) = \bar{\mathbf{u}}(\xi, \eta) + \mathbf{U}(\xi, \eta, \zeta) \quad (5)$$

$$\bar{\mathbf{u}}(\xi, \eta) = \sum_{a=1}^n N_a(\xi, \eta) \bar{\mathbf{u}}_a \quad (6)$$

$$\mathbf{U}(\xi, \eta, \zeta) = \sum_{a=1}^n N_a(\xi, \eta) \frac{h_{ka}}{2} \zeta \hat{\mathbf{U}}_a \quad (7)$$

$$\bar{\mathbf{u}}_a = \{\bar{u}_{a1} \quad \bar{u}_{a2} \quad \bar{u}_{a3}\}^T; \hat{\mathbf{U}}_a = \theta_{a2} \mathbf{e}_{a1}^f - \theta_{a1} \mathbf{e}_{a2}^f \quad (8)$$

The quantities  $\theta_{a1}$  and  $\theta_{a2}$  respectively represent the rotations of the fiber about the basis vectors  $\mathbf{e}_{a1}^f$  and  $\mathbf{e}_{a2}^f$  of the fiber coordinate system at node  $a$ . From Eq. (8) it is apparent that the K-Shell element has five degrees of freedom for each node.

Using the displacement approximation given by Eqs. (5)-(8), the element mapping given by Eqs. (2)-(4), the variational equation Eq. (1), and employing the standard formulation procedure of the FEM (see e.g. [13,14,15]) lead to the dynamic equilibrium equation for each shell element as follows

$$\mathbf{m}\ddot{\mathbf{d}} + \mathbf{k}\mathbf{d} = \mathbf{f} \quad (9)$$

where  $\mathbf{m}$  is the element consistent mass matrix,  $\mathbf{k}$  is the element stiffness matrix,  $\mathbf{d}$  is the element nodal displacement vector,  $\ddot{\mathbf{d}}$  is the element nodal acceleration vector and  $\mathbf{f}$  is the element nodal force vector. The order of these matrices depends on the number of nodes in the support domain,  $n$ , and it may vary from element to element. The global discretized equation for dynamic analyses of shell structures can be obtained from the elemental discretized equation, Eq. (9), by using the assembly procedure. Here the assembly process for each element involves all nodes in the element's support domain,  $n$ , not only the nodes within the element as in the conventional FEM. For static cases, Eq. (9) simply reduces to  $\mathbf{k}\mathbf{d} = \mathbf{f}$ .

### 3. Testing of the K-Shell

#### 3.1. Modified pinched cylinder with end diaphragms

The problem is a short circular cylinder with rigid end diaphragms subjected to two pinching forces as shown in Fig. 2. Taking advantage of the symmetry, only one octant of the cylinder is needed in the analysis. The original problem has a constant thickness of  $h=3$  unit. The reference solution for the deflection of the points where the forces act is  $1.8248 \times 10^{-5}$  [16]. The K-Shell has been tested to this challenging problem and it was found that the results converged monotonically from below to the reference solution [11].

For the purpose of the present test, the thickness of the cylinder was modified so that it varies linearly from  $h=3$  along the side of A-A to  $h=15$  along the side of B-B and C-C (see Fig. 2). The octant of the cylinder was analysed using meshes  $4 \times 4, 8 \times 8, 16 \times 16$ , and  $32 \times 32$  elements. In order to obtain a reference solution for the modified cylinder, it was analysed using two different 20-node continuum brick elements C3D20 and C3D20RH of Abaqus with the mesh of  $32 \times 32$ . The C3D20 is the standard 20-node brick element, whereas the C3D20RH is the 20-node brick element with reduced integration and hybrid formulation [17]. The C3D20 and C3D20RH results for the deflection at the point where the force acts are  $7.173 \times 10^{-7}$  and  $7.578 \times 10^{-7}$ , respectively. The average of these results was taken as the reference solution.

The K-Shell results were presented in Table 1 together with their normalized values with respect to the reference solution. The table indicates that, as expected, the K-Shell solutions converge monotonically from below to the reference solution. The errors of the solution, i.e. the difference between the solutions to the reference solution, were plotted against the number of elements for each side,  $M$ , in the log-log scale as shown in Fig. 3. The average

convergence rate is 2.36, which is lower than the theoretically optimal convergence rate of the K-Shell, i.e. 5. The possible reason for the slow convergence of the K-Shell is that the shear and membrane locking phenomena. In addition, the displacement field contains highly localized displacement in the vicinity of the applied force [10,11].

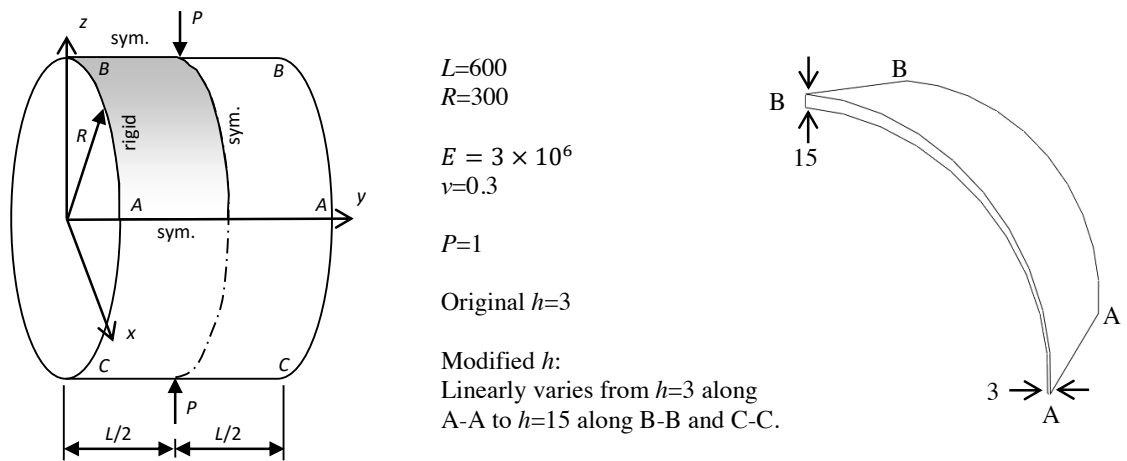


Fig. 2. (a) Pinched cylinder with rigid end diaphragms; (b) An octant of the modified pinched cylinder.

### 3.2. Modified hemispherical shell with $18^\circ$ cut-off

A hemispherical shell structure with  $18^\circ$  cut-off is subjected to four equal forces alternating in directions, inward and outward, around its equator. Due to symmetry, only one quarter of the hemisphere is needed in the analysis (Fig. 4). The original problem has a constant thickness of  $h=0.04$  unit. The reference solution for the deflection of the points where the forces act is 0.0935 [10]. The K-Shell has been tested to this problem and, like in the previous problem, the results converged monotonically from below to the reference solution [10].

For the purpose of the present study, the thickness of the hemispherical shell was modified as shown in Fig. 4(b). The quarter of the modified shell was analysed using meshes with different degrees of refinement, i.e. from  $4 \times 4$  to  $32 \times 32$  elements. The deflections at the points where the forces act obtained using the C3D20 and C3D20RH elements of Abaqus with the mesh of  $32 \times 32$  are  $7.609 \times 10^{-5}$  and  $7.659 \times 10^{-5}$ , respectively. The average of these results, i.e.  $7.634 \times 10^{-5}$ , was taken as the reference solution.

The results obtained from the analysis using the K-Shell were presented in Table 2. It is seen that the results converge to the reference solution. Fig. 5 shows that the convergence rate decreases as the mesh was refined. The average convergence rate is 1.49, which is also lower than the theoretical convergence rate of the K-Shell, 5, for the same reason as in the case of the pinched cylinder.

Table 1. Results of the K-Shell for the modified cylinder.

M	Deflection	Normalized Deflection
4	2.392E-07	0.32
8	6.167E-07	0.84
16	6.584E-07	0.89
32	7.412E-07	1.00
*Ref.	7.376E-07	1.00

M: Number of elements on each side  
 \*The average of C3D20 and C3D20RH results for M=32

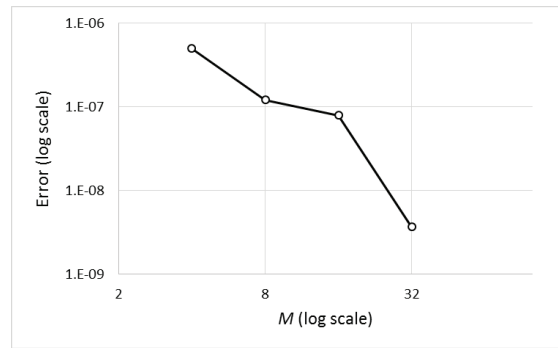
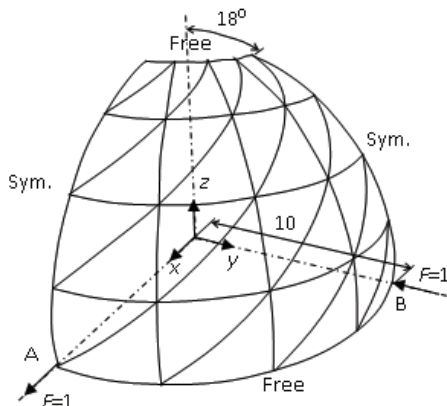


Fig. 3. Error vs number of elements on each side.



$$E = 68.25 \times 10^6$$

$$\nu = 0.3$$

Original  $h=0.04$ ;  $R/h=250$

Modified  $h$ :  
 Linearly varies from  $h=0.04$   
 along the top edge to  $h=0.5$   
 ( $R/h=20$ ) along the equator.

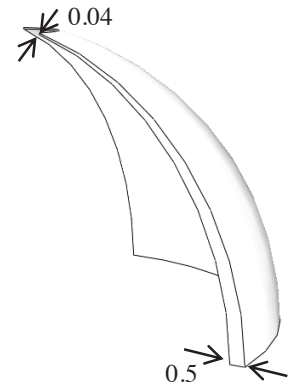


Fig. 4. (a) A quarter of the hemispherical shell modelled with 4x4 K-Shell elements; (b) A quarter of the shell with modified thickness.

Table 2. Results of the K-Shell for the modified hemispherical shell.

M	Deflection	Normalized Deflection
4	9.150E-06	0.12
8	6.440E-05	0.84
16	7.200E-05	0.94
32	7.330E-05	0.96
*Ref.	7.634E-05	1.00

M: Number of elements on each side  
 \*The average of C3D20 and C3D20RH results for M=32

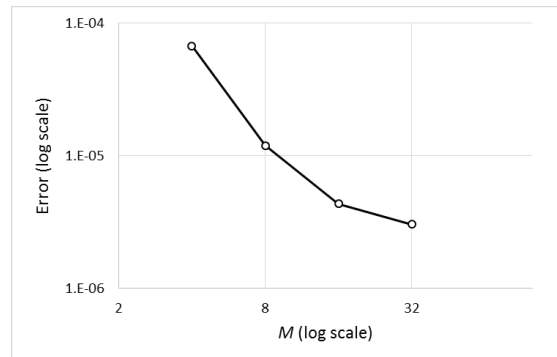


Fig. 5. Error vs number of elements on each side.

#### 4. Conclusions

An overview of the formulation of the recently developed Kriging-based shell element, K-Shell, and the numerical tests using two modified problems of the well-known benchmark problems, namely the varying-thickness

pinched cylinder and the varying-thickness hemispherical shell, have been presented. The tests showed that the results converged to the reference solutions obtained from the three-dimensional elements of commercial software Abaqus and it thus confirmed the K-Shell capability in analyzing shell structures with varying thickness. The convergence rates of the K-Shell results, however, were not optimum. The possible reason for this is that membrane locking and/or shear locking were severe in the tests problems. For improvement of the K-Shell performance, future research should be directed to make the K-Shell free from both the shear locking and the membrane locking.

## References

- [1] K. Plengkhom, W. Kanok-Nukulchai, "An enhancement of finite element method with moving Kriging shape functions," *Int. J. Comput. Methods*. 02 (2005) 451–475.
- [2] F. T. Wong, W. Kanok-Nukulchai, "Kriging-based finite element method: element-by-element Kriging interpolation," *Civ. Eng. Dimens.* 11 (2009) 15–22.
- [3] W. Kanok-Nukulchai, F. T. Wong, "A break-through enhancement of FEM using node-based Kriging Interpolation," *IACM Expressions*, IACM, Barcelona, 2008, pp. 24–29.
- [4] F. T. Wong, W. Kanok-Nukulchai, "On the convergence of the Kriging-based finite element method," *Int. J. Comput. Methods*. 06 (2009) 93–118.
- [5] T. Q. Bui, M. N. Nguyen, C. Zhang, "A moving Kriging interpolation-based element-free Galerkin method for structural dynamic analysis," *Comput. Methods Appl. Mech. Eng.* 200 (2011) 1354–1366.
- [6] T. Q. Bui, M. N. Nguyen, "A moving Kriging interpolation-based meshfree method for free vibration analysis of Kirchhoff plates," *Comput. Struct.* 89 (2011) 380–394.
- [7] T. Q. Bui, M. N. Nguyen, C. Zhang, "Buckling analysis of Reissner–Mindlin plates subjected to in-plane edge loads using a shear-locking-free and meshfree method," *Eng. Anal. Bound. Elem.* 35(2011) 1038–1053.
- [8] L. Gu, "Moving Kriging interpolation and element-free Galerkin method," *Int. J. Numer. Methods Eng.* 56 (2003) 1–11.
- [9] F. T. Wong, W. Kanok-Nukulchai, "A Kriging-based finite element method for analyses of shell structures," in *Proceedings of the Eighth World Congress on Computational Mechanics and the Fifth European Congress on Computational Methods in Applied Sciences and Engineering*, 2008, ECCOMAS, p. a1247.
- [10] F. T. Wong, "Kriging-based finite element method for analyses of plates and shells," dissertation, Asian Institute of Technology, Pathumthani, 2009.
- [11] F. T. Wong, "Testing of shell elements using challenging benchmark problems," in *Proceedings of the 2nd Indonesian Structural Engineering and Materials Symposium*, 2013, Parahyangan Catholic University, Bandung, pp. T10–1–T10–11.
- [12] "Abaqus Overview - Dassault Systèmes." [Online]. Available: <http://www.3ds.com/products-services/simulia/portfolio/abaqus/overview/>. [Accessed: 01-Oct-2013].
- [13] T. J. R. Hughes, *The Finite Element Method: Linear Static and Dynamic Finite Element Analysis*, Prentice-Hall, New Jersey, 1987.
- [14] R. D. Cook, D. S. Malkus, M. E. Plesha, R. J. Witt, *Concepts and Applications of Finite Element Analysis*, fourth ed., John Wiley & Sons, 2002.
- [15] O. C. Zienkiewicz, R. L. Taylor, *The Finite Element Method, Volume 1: The Basis*, fifth ed., Butterworth-Heinemann, Massachusetts, 2000.
- [16] T. Belytschko, H. Stolarski, W. K. Liu, N. Carpenter, J. S. J. Ong, "Stress Projection for Membrane and Shear Locking in Shell Finite Elements," *Comput. Methods Appl. Mech. Eng.* 51(1985) 221–258.
- [17] "Abaqus Theory Manual." Dassault Systemes Simulia Corp., Providence, 2009.